JGR Atmospheres

RESEARCH ARTICLE
10.1029/2023JD039385

Mechanisms of Added Value of a Coupled Global Ocean-Regional Atmosphere Climate Model Over Central Equatorial Africa

Alain T. Tamoffo[1], Torsten Weber[1], William Cabos[2], Dmitry V. Sein[3,4], Alessandro Dosio[5], Diana Rechid[1], Armelle R. Remedio[1], and Daniela Jacob[1]

[1]Climate Service Center Germany (GERICS), Helmholtz-Zentrum Hereon, Hamburg, Germany, [2]Departamento de Física Y Matemáticas, Universidad de Alcalá, Alcalá de Henares, Madrid, Spain, [3]Alfred Wegener Institute for Polar and Marine Research, Bremerhaven, Germany, [4]Shirshov Institute of Oceanology, Russian Academy of Science, Moscow, Russia, [5]European Commission, Joint Research Centre (JRC), Ispra, Italy

Abstract There is an urgent need to enhance climate projections for Central Equatorial Africa (CEA), given the region's high vulnerability to climatic hazards and its economy's heavy dependence on climate-sensitive sectors. This study aims to evaluate the performance of the regional earth system model ROM, composed of the atmosphere-only regional climate model (RCM) REMO coupled with the global Max Planck Institute for Meteorology Ocean Model (MPIOM), in reproducing the precipitation climatology over CEA. ROM results are compared to those of REMO in two sets of experiments, one driven by the ERA-Interim reanalysis and the other by the MPI-ESM-LR earth system model (ESM), both at ~25-km horizontal resolution. Results show that ocean coupling improves rainfall climatology thanks to a better representation of the physical processes and mechanisms underlying the rainfall system. In particular, an improved sea surface temperature (SST) results in a more realistic simulation of land-atmosphere-ocean interactions, and subsequently the atmospheric baroclinicity. Specifically, the coupling reduces the positive SST bias inherited by the driving ESM across the entire Guinea Gulf and Benguela-Angola coastal seas. This leads to better simulated land-ocean thermal and pressure contrasts. Improvements in land-ocean contrasts, in turn, enhance the representation of the regional atmospheric circulation, and thus precipitation. Interestingly, the coupling is more beneficial when ROM is driven by the ESM than the reanalysis. This study emphasizes the advantage of dynamically downscaling ESMs using regional earth system models rather than atmosphere-only RCMs, with the potential to enhance confidence in future climate projections.

Plain Language Summary Designing timely and relevant societal responses to climate-related impacts and risks to humans and natural systems requires reliable information about climate variability and projected change, especially at regional scales. For this purpose, considerable efforts were devoted to the improvement of the numerical models used to represent the climate system, including better formulation of the models' physical and dynamical components and the inclusion of feedback between different components of the climate systems, such as those between the ocean and the atmosphere. In this study we aim at investigating whether the use of a regional climate model which includes an explicit representation (coupling) of the ocean is able to better simulate (i.e., adds value) the main mechanisms responsible for precipitation over Central Equatorial Africa. The results show that the coupled model is indeed able to simulate more realistically the complex physical processes and mechanisms underpinning the rainfall system. Our findings advocate for the use of the global ocean-regional atmosphere coupling approach for regional climate change projection analyses.

Key Points:

- The global ocean-regional atmosphere coupling improves the rainfall climatology compared to its atmosphere-only counterpart model
- The added value resulting from the coupling is plausible, as associated with improvements in the processes underpinning the rainfall system
- The added value is modulated by the boundary conditions, with better suitability under the imperfect forcing mode

Supporting Information:

Supporting Information may be found in the online version of this article.

Correspondence to:

A. T. Tamoffo,
Alain.Tamoffo@hereon.de;
alaintamoffotchio@gmail.com

Citation:

Tamoffo, A. T., Weber, T., Cabos, W., Sein, D. V., Dosio, A., Rechid, D., et al. (2024). Mechanisms of added value of a coupled global ocean-regional atmosphere climate model over Central Equatorial Africa. *Journal of Geophysical Research: Atmospheres*, *129*, e2023JD039385. https://doi.org/10.1029/2023JD039385

Received 7 SEP 2023
Accepted 20 JAN 2024

Author Contributions:

Conceptualization: Alain T. Tamoffo, Torsten Weber, William Cabos, Dmitry V. Sein
Data curation: Alain T. Tamoffo
Formal analysis: Alain T. Tamoffo, Torsten Weber, Alessandro Dosio, Armelle R. Remedio
Funding acquisition: Daniela Jacob
Investigation: Alain T. Tamoffo
Methodology: Alain T. Tamoffo, Torsten Weber, William Cabos, Dmitry V. Sein, Alessandro Dosio

© 2024. The Authors.
This is an open access article under the terms of the Creative Commons Attribution License, which permits use, distribution and reproduction in any medium, provided the original work is properly cited.

1. Introduction

The dynamical downscaling of Earth system models (ESMs) by means of regional climate models (RCMs) has significantly improved the numerical representation of the African climate system (Crétat et al., 2013; Dosio et al., 2015; Gibba et al., 2018; Giorgi & Gutowski, 2015; Hernández-Díaz et al., 2016; Laprise et al., 2013; Paxian et al., 2016; Sylla et al., 2012). This is most often highlighted with the reference to the reduction of uncertainties in climate simulations, especially for indices of extreme weather and climate events over the continent (Dosio et al., 2019, 2021b; Haensler et al., 2011; Hernández-Díaz et al., 2016; Weber et al., 2018). However, despite these significant advances, substantial biases remain in the downscaled results even when driven by

Project Administration: Torsten Weber, Daniela Jacob
Resources: Torsten Weber, Diana Rechid, Daniela Jacob
Software: Alain T. Tamoffo, Torsten Weber
Supervision: Torsten Weber, William Cabos, Dmitry V. Sein, Alessandro Dosio, Diana Rechid
Validation: Alain T. Tamoffo, Torsten Weber, William Cabos, Dmitry V. Sein, Alessandro Dosio, Diana Rechid, Armelle R. Remedio, Daniela Jacob
Visualization: Alain T. Tamoffo, Torsten Weber, William Cabos, Dmitry V. Sein, Diana Rechid, Armelle R. Remedio, Daniela Jacob
Writing – original draft: Alain T. Tamoffo, Torsten Weber
Writing – review & editing: Alain T. Tamoffo, Torsten Weber, William Cabos, Dmitry V. Sein, Alessandro Dosio, Diana Rechid, Armelle R. Remedio, Daniela Jacob

quasi-perfect boundary conditions (reanalysis) (Laprise et al., 2013; Nikulin et al., 2012; Panitz et al., 2014). Central equatorial Africa (CEA) is one of the world's regions where RCMs still struggle to represent the rainfall system (Fotso-Kamga et al., 2020; Fotso-Nguemo et al., 2016, 2019; Haensler et al., 2013; Tamoffo, Vondou, et al., 2019, 2021,2022). Results of RCMs are indeed characterized by large biases for both hindcasts and historical simulations as well as by large ranges of uncertainty in their projections (Taguela et al., 2020; Tamoffo, Moufouma-Okia, et al., 2019, 2020). Such a situation is detrimental to the use of model results especially for climate change-related risk assessment.

Considerable efforts have been devoted to improve the models' simulations of the African climate system. Some works (e.g., Wu et al., 2020) argued that over Africa the model physical parameterization significantly affects the precipitation spatiotemporal patterns whereas the increased horizontal resolution only influences the intensity. Other works (Sørland et al., 2021) claimed that boundary conditions may affect the results more critically than model version, configuration and horizontal resolution. Other studies (e.g., Hernández-Díaz et al., 2016; Hoffmann et al., 2016) attempted to adjust the sea surface temperature (SST) prior to the downscaling in order to reduce inherited errors from driving boundary conditions. Weber et al. (2022) argued that although this approach is fruitful in improving hindcast and historical simulations, it may induce inadequacies in the response of the lower atmosphere processes to the SST in future climates. These findings highlight that improvements in the representation of underlying physical processes and mechanisms are paramount for a plausible simulation of rainfall climatology over CEA (Tamoffo et al., 2021).

A more recent approach consists in coupling an RCM with a global ocean model (Samanta et al., 2018; Sein et al., 2015; Zou & Zhou, 2016) to allow fully coupled ocean-atmosphere-land feedback. Unlike the usual atmosphere-only dynamical downscaling approach applied in the Coordinated Regional Climate Downscaling Experiment (CORDEX; Giorgi & Gutowski, 2015) as well as the downscaling after SST bias-adjustment, the coupling accounts explicitly for the feedback between different Earth system components. In addition, as the precipitation system is strongly correlated with SST over equatorial Africa (Balas et al., 2007; Dezfuli & Nicholson, 2013), a realistic simulation of precipitation would be afore-conditioned by a realistic simulation of SST. It is noteworthy that the reverse may also be true because the causal relationship between the oceanic forcings and the regional convective system has not yet been elucidated.

Coupled atmosphere-ocean RCMs have been proven fruitful in improving the representation of the climate system in northern North Atlantic and Europe (Sein et al., 2015), southern Africa (Ratnam et al., 2015), East Asia (Zou & Zhou, 2016), and West Africa (Paxian et al., 2016). Similar conclusions have recently been drawn for CEA by Weber et al. (2022), although they did not elucidate the reasons behind the models' improvement. Evaluating the plausibility of the added value in such a region, which is characterized by a shortage of ground station measurements, is absolutely needed to attest to the credibility of the models representing the regional climate system. This argument is supported by previous research by James et al. (2017) and by the sixth report of the Intergovernmental Panel on Climate Change (IPCC's AR6 Ch 10; Doblas-Reyes et al., 2021), who argued that performance-based evaluation of climate models should be priorly associated with a process-oriented assessment, especially in regions featuring coarse observed networks like CEA.

Therefore, the present study aims to address the following concerns.

1. Is the added value of a coupled global ocean-regional atmosphere RCM with respect to the corresponding atmosphere-only RCM, associated with a more realistic representation of the relevant underlying physical mechanisms over CEA?
2. Is this added value modulated by the boundary conditions? Otherwise, is the coupled RCM's improvement systematic?

By answering the above questions, we hope to support the development of RCMs in better simulating the equatorial African climate system. Moreover, this study is intended to stimulate discussion on the appropriateness of using coupled RCMs rather than atmosphere-only RCMs to assess climate projections for CEA. The following section describes experimental, observational and reanalysis data and the methods used in this study. Section 3 intercompares coupled against uncoupled RCMs of rainfall climatology and related added value. In Section 4, the mechanisms associated with the added value of using the coupled ocean-atmosphere model are investigated and the credibility of each RCM simulation group is highlighted. Section 5 discusses and wraps up the findings.

21698996, 2024, 3, Downloaded from https://agupubs.onlinelibrary.wiley.com/doi/10.1029/2023JD039385 by Alfred Wegener Institut F. Polar- U. Meeresforschung Awi, Wiley Online Library on [30/10/2024]. See the Terms and Conditions (https://onlinelibrary.wiley.com/terms-and-conditions) on Wiley Online Library for rules of use; OA articles are governed by the applicable Creative Commons License

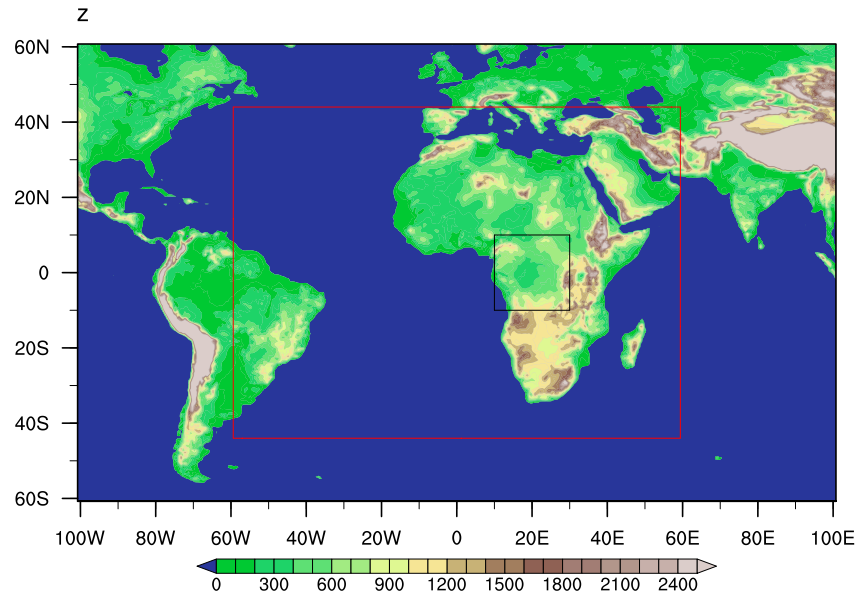

Figure 1. The coupling area (red box), along with the domain topography (in Meter) from the NASA GTOPO30. Also shown is the CEA area (black box).

2. Data and Methods

2.1. Data

In this study, we employ both the atmosphere-only (i.e., uncoupled) Regional Climate Model REMO (Jacob, 2001), and the regionally-coupled model ROM (Sein et al., 2015), which is the combination of REMO with the Max Planck Institute Ocean Model (MPIOM; Jungclaus et al., 2013). Hereafter, the term REMO will be used when referring to the uncoupled simulations, while the term ROM will be used for the coupled simulations. Detailed descriptions of REMO and ROM used in various configurations are found in several previous studies (Cabos et al., 2020; Jacob et al., 2012; Sein et al., 2014). The physical configurations used in the present work and model spin up are extensively described in Weber et al. (2022) and therefore, will not be repeated here. The coupling zone (red box) is depicted in Figure 1, along with the topography of the domain. The experimental designs consist of two forcing configurations: (a) the quasi-perfect forcing configuration, where lateral boundary conditions are extracted from the European Center for Medium-Range Weather Forecasts (ECMWF) ERA-Interim reanalysis data (Dee et al., 2011) and (b) the imperfect forcing configuration, with lateral boundary conditions from the Max Planck Institute ESM lower resolution (MPI-ESM-LR; Stevens et al., 2013). As both MPI-ESM-LR and ROM share the same ocean component, and, in addition, both REMO and ROM are based on the same physical parameterizations and dynamical core as ECHAM (which is the atmospheric component of MPI-ESM-LR; Jacob et al., 2012), this minimizes inconsistencies between the forcing and the downscaling models. More details about the driving ESM and reanalysis are shown in Table 1.

The results of the first configuration are helpful to discern the impact of the coupling without the influence of ESMs' biases on the boundary conditions. It should be noted that in this case, REMO is forced on the ocean surface by SST derived from ERA-Interim and is therefore more constrained to the reanalysis than ROM. Conversely, ROM's

Table 1
Details of Forcing Data and Names of RCM Experiments Used in This Study

Institution	ESMs' names	RCMs (0.22° × 0.22°)	Experiment names	Ocean-atmosphere	Periods used	References
European Center for Medium Range Weather Forecasts	ERA (0.75° × 0.75°)	REMO	REMO-ERA	Uncoupled	1980–2005	Dee et al. (2011)
		ROM	ROM-ERA	Coupled		
Max Planck Institute for meteorology	MPI-ESM-LR (1.9° × 1.9°)	REMO	REMO-MPI-ESM-LR	Uncoupled	1980–2005	Stevens et al. (2013)
		ROM	ROM-MPI-ESM-LR	Coupled		

21698996, 2024, 3, Downloaded from https://agupubs.onlinelibrary.wiley.com/doi/10.1029/2023JD039385 by Alfred Wegener Institut F. Polar- U. Meeresforschung Awi, Wiley Online Library on [30/10/2024]. See the Terms and Conditions (https://onlinelibrary.wiley.com/terms-and-conditions) on Wiley Online Library for rules of use; OA articles are governed by the applicable Creative Commons License

Table 2
Description of Reanalysis and Satellite/Gauge Data Sets Employed for the Inter-Comparison Analysis

Data Set	Institution	Horizontal resolution	Periods used	Reference
CRU-TS4.05	Center for Atmospheric Research (NCAR)Climate Research Unit, University of East Anglia	0.5° × 0.5°	1980–2005	Harris et al. (2020)
GPCC-v2020	Global Precipitation Climatology Center	0.25° × 0.25°	1980–2005	Schneider et al. (2022)
CHIRPS2	Climate Hazards InfraRed Precipitation with Stations	0.05° × 0.05°	1980–2005	Funk et al. (2015)
ERA5/ERA-Interim	European Center for Medium-Range Weather Forecasts	0.25° × 0.25°/0.75° × 0.75°	1980–2005	Hersbach et al. (2020)/ Dee et al. (2011)
MERRA2	The Modern-Era Retrospective analysis for Research and Application, version 2	0.5° × 0.66°	1980–2005	NASA (2016)

atmospheric fields can be affected by the biases induced by the coupling and the oceanic component, but benefit from the more physical representation of heat and mass fluxes that bring the interactive SST (usually over the ocean). The second configuration aims to highlight whether the coupling is able to improve the model's results when driven by lateral boundary conditions and, consequently, affected by biases from the driving ESM. In this case, the REMO simulation is also influenced by the biases in the ESM SST. On the other hand, for grid points distant from the boundaries, ROM SST is less influenced by the driving ESM (Sein et al., 2014), and hence, there is a potential for ROM to simulate SST better than the ESM resulting in modeled precipitation being closer to observations.

Several reference datasets are used to evaluate the ability of ROM to improve simulated atmospheric fields against REMO. Indeed, over CEA, the network of in situ stations is very sparse. Consequently, observational datasets are generally the result of a combination of gauge and satellite measurements, as well as reanalysis models. Using multiple sources of reference is therefore required to account for uncertainties in these products (Dosio, Pinto, et al., 2021). The full list and details of the baseline data used throughout the study are summarized in Table 2.

2.2. Methods

The performance-based evaluation of both coupled and uncoupled experiments is first performed against reference datasets, and, then, the two simulation groups are intercompared with each other. The performance metrics used for the evaluation are the mean bias (at 95% statistically significant level using the Student *t*-test) and the added value (*AV*). For the bias and *AV* computation, we remapped the RCM results onto the observation or reanalysis grid used as reference, apart from the CHIRPS2 dataset, which was instead re-gridded to match the model's grid because of its higher horizontal grid spacing (0.05° × 0.05°) compared to that of the RCM (0.22° × 0.22°).

In our analysis, the added value does not measure the performance of RCM runs against the driving ESM or reanalysis (Di Luca et al., 2012; Dosio et al., 2015), but rather, directly compares the performance of ROM with regards to REMO in representing the climatology of precipitation. The AV is defined as in Dosio et al. (2015) following the expression:

$$AV = \frac{(X_{REMO} - X_{ref})^2 - (X_{ROM} - X_{ref})^2}{Max\left((X_{REMO} - X_{ref})^2, (X_{ROM} - X_{ref})^2\right)} \quad (1)$$

where X represents the spatial distribution of the considered experiment. Values are normalized by their maximum (Max) so that $-1 \leq AV \leq 1$. Thus defined, a positive AV means that the ROM coupled simulation improves over the REMO uncoupled simulation and vice versa.

To explore the reasons behind the sign of AV, we examined physical processes and mechanisms that have been already highlighted in the literature as drivers of the CEA rainfall system. These include SST (Balas et al., 2007; Dezfuli & Nicholson, 2013; Nicholson & Dezfuli, 2013), low-level westerlies (LLWs; Pokam et al., 2014), the African easterly jets (AEJs) defined as mid-tropospheric (700–600 hPa) easterly wind speeds exceeding 6 m/s (Chen, 2005; Kuete et al., 2019), and, finally, the Congo basin cell (CBC) estimated by means of the zonal mass-weighted streamfunction (Longandjo & Rouault, 2020):

$$\Psi_Z(P) = \frac{2\pi R}{g} \int_{sp}^{P} [u] dp \quad (2)$$

21698996, 2024, 3, Downloaded from https://agupubs.onlinelibrary.wiley.com/doi/10.1029/2023JD039385 by Alfred Wegener Institut F. Polar- U. Meeresforschung Awi, Wiley Online Library on [30/10/2024]. See the Terms and Conditions (https://onlinelibrary.wiley.com/terms-and-conditions) on Wiley Online Library for rules of use; OA articles are governed by the applicable Creative Commons License

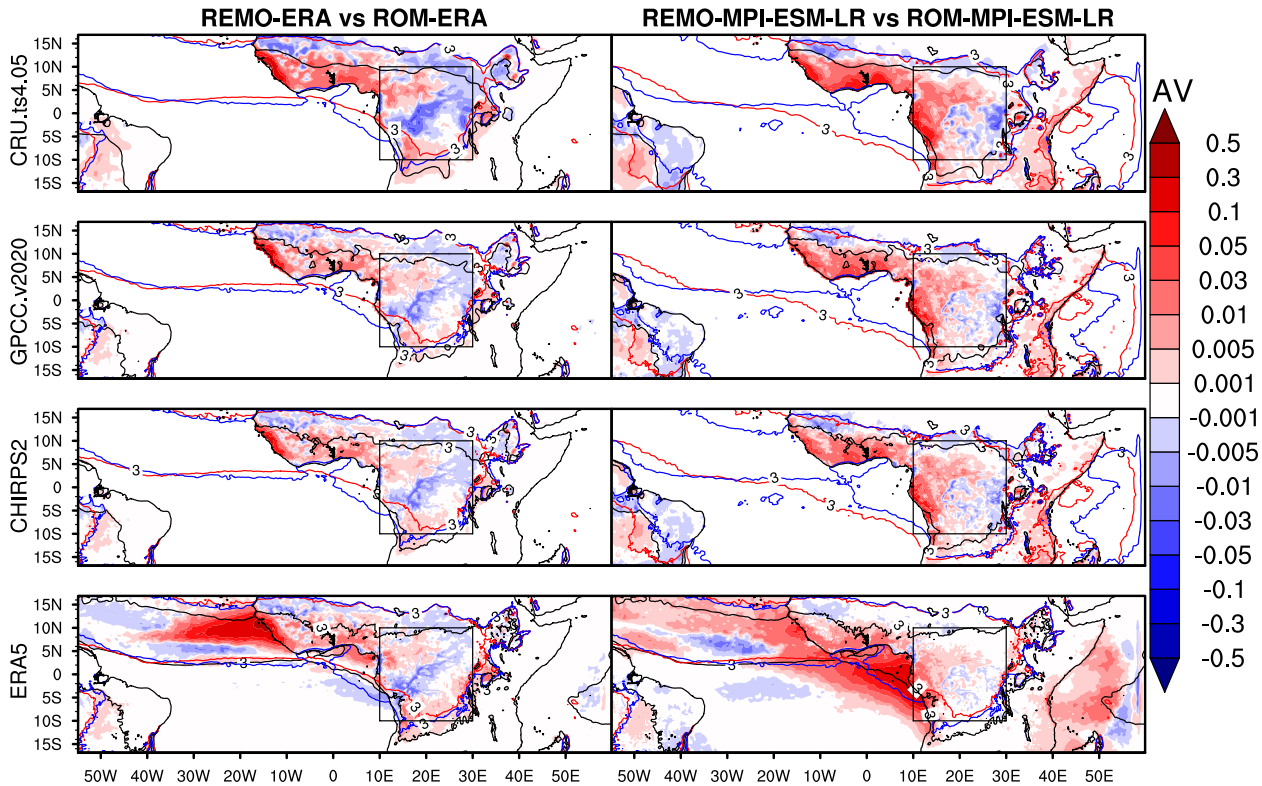

Figure 2. Added value (AV) of mean SON CEA precipitation in REMO compared to ROM experiments. The reference datasets used are CHIRPS2, CRU.ts.05, GPCC-v2020 and ERA5, over the period 1981 to 2005. Positive (negative) values indicate a lower (higher) precipitation bias of ROM compared to REMO. Contours indicate the position of the rain-band (i.e., precipitation larger than 3 mm/day) from the reference dataset (black), REMO (red) and ROM (blue). The black box denotes CEA.

where R is the Earth's radius, g the constant of gravity, sp the surface pressure and $P \in$ [1,000–500 hPa], while the operator [ ] signifies a zonal average.

It is important to note that September-October-November (SON) is the wettest season over CEA (defined as 10°S–10°N; 10°–30°E, see black box in Figure 1) and the time of year when most of the processes that underpin the rainfall system are active (Jackson et al., 2009; Nicholson & Grist, 2003). As the scope of our study is to evaluate how models represent not only the precipitation climatology of the region, but also the mechanisms mainly responsible for it, our analysis focuses on SON only.

3. The Uncoupled REMO Versus Coupled ROM: The Added Value

Figure 2 shows the *AV* of seasonal mean precipitation as simulated by REMO versus ROM using three observational datasets (CRU.ts4.05, GPCC.v2020, and CHIRPS2) as reference. The result of the *AV* relative to ERA5 is also shown since this reanalysis is used as the benchmark for diagnosing mechanisms associated with *AV*. At first sight, the overall *AV* spatial pattern (and that of the mean bias, not shown) does not depend on the dataset used as reference. The observational uncertainties do not significantly affect the *AV*: in fact, the difference between *REMO* and *ROM* results when driven by either the reanalysis or the ESM are greater than the observational uncertainty. Indeed, when they are run under the near-perfect forcing configuration, there is little difference between REMO and ROM results in terms of the number of grid points where there is an improvement or a deterioration (Figure 3a). In this case, the *AV* spatial pattern mainly shows positive values over northwestern and southeastern CEA and negative (or very small) ones elsewhere (Figure 2). This leads to generally equal or close performance between REMO and ROM (Figure 3a). Moreover, there is no clear sign of improvement or deterioration in the Guinea Gulf (Figure 2) where atmospheric-only RCMs generally exhibit strong wet/dry biases (Laprise et al., 2013; Dosio & Panitz, 2015; Fotso-Nguemo et al., 2016; Tamoffo, Moufouma-Okia, et al., 2019, 2022; also see Fig. S1 in Supporting Information S1). The coupled and uncoupled experiments greatly extend the rain-band northwards compared to reference datasets, but instead, narrow it slightly along the southern side of the

21698996, 2024, 3, Downloaded from https://agupubs.onlinelibrary.wiley.com/doi/10.1029/2023JD039385 by Alfred Wegener Institut F. Polar- U. Meeresforschung Awi, Wiley Online Library on [30/10/2024]. See the Terms and Conditions (https://onlinelibrary.wiley.com/terms-and-conditions) on Wiley Online Library for rules of use; OA articles are governed by the applicable Creative Commons License

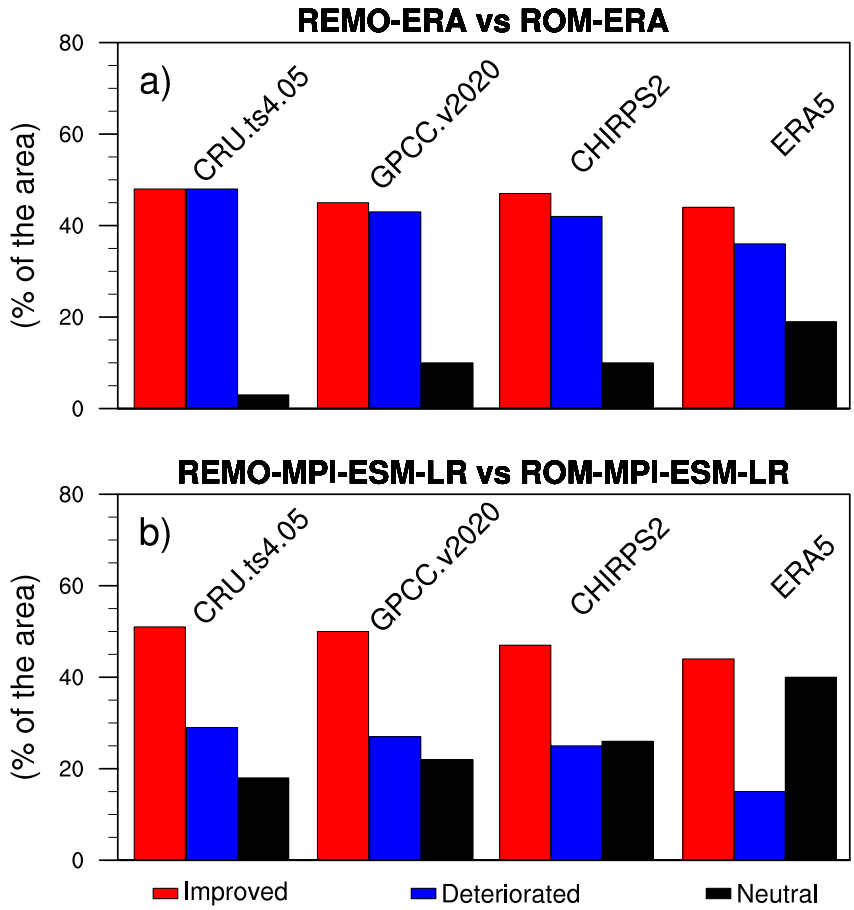

Figure 3. Percentage of improvement (AV > 0.001), deterioration (AV < −0.001) and neutral (−0.001 ≤ AV ≤ +0.001) of REMO and ROM experiments relative to CRU.ts.05, GPCC-v2020, CHIRPS2 and ERA5, over the period 1980 to 2005.

rain-band. However, when run under imperfect forcing configuration, that is, forced with MPI-ESM-LR, ROM outperforms REMO over CEA and even in the Guinea Gulf (Figure 2), in agreement with the strong reduction of the wet bias over oceanic regions by the coupled simulation (Fig. S1 in Supporting Information S1). In this case, the area of improvement is most often almost twice as large (or more for ERA5) than the area of deterioration (Figure 3b). The *AV* spatial pattern consists of improvements along the coastal areas and in the northern part of the CEA, but rather heterogeneous areas featuring elsewhere. With respect to improvements in simulated precipitation climatology, the coupling generally attenuates the magnitude of the rainfall bias. While comparing REMO-MPI-ESM-LR and ROM-MPI-ESM-LR, it appears that the coupling significantly reduces the intensity of the wet bias over oceanic and coastal areas of the Guinea Gulf (Fig. S1 in Supporting Information S1). In this case, the coupling acts in improving the location of the rain-band, especially along the southern side of the rain-band over the ocean. This offers an opportunity to understand the reasons behind overestimated precipitation over this region, usually modeled by atmospheric-only RCMs.

The above results are logical in that the ocean-atmosphere coupling appears to be more advantageous under imperfect forcing than under quasi-perfect forcing configuration. Indeed, when forced by ERA-Interim, the coupling does not substantially change the precipitation pattern over the ocean (Fig. S1 in Supporting Information S1). ROM, in contrast, substantially reduces the magnitude of rainfall wet biases over the ocean when driven by the MPI-ESM-LR ESM, compared to REMO. In this case, the coupling may have improved the bias inherited from MPI-ESM-LR through the boundary conditions. This assumption seems likely given that MPI-ESM-LR simulates, for instance, more biased SSTs than ERA-Interim (Figure 4). In case this assumption is attested, the dynamical downscaling by means of a coupled ocean-atmosphere RCM would therefore result beneficial especially in regions where the climate system is greatly influenced by the land-sea interaction and feedback (such as CEA), and where ESMs can show large SST biases (e.g., Creese & Washington, 2018; Kuete et al., 2022; Taguela

21698996, 2024, 3, Downloaded from https://agupubs.onlinelibrary.wiley.com/doi/10.1029/2023JD039385 by Alfred Wegener Institut F. Polar- U. Meeresforschung Awi, Wiley Online Library on [30/10/2024]. See the Terms and Conditions (https://onlinelibrary.wiley.com/terms-and-conditions) on Wiley Online Library for rules of use; OA articles are governed by the applicable Creative Commons License

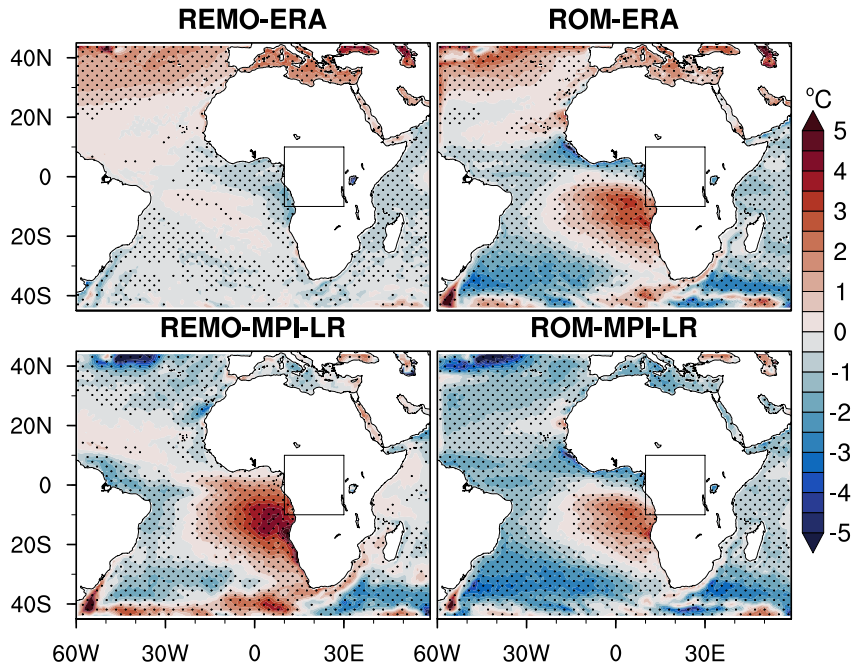

Figure 4. Mean (1980–2005) SON SST biases (REMO/ROM minus ERA5). The biases are computed relative to ERA5 reanalysis. The stipples occur where the difference between the dataset under consideration and the ERA5 reanalysis dataset is statistically significant at the 95% confidence level by means of the Student's *t*-test. The black boxes indicate the CEA.

et al., 2022). To this, it is critically important to assess the plausibility of the *AV* resulting from the coupling. Therefore, in the following sections we intercompare REMO and ROM in representing the physical processes and mechanisms that underpin the CEA rainfall system. The ERA5 reanalysis is used as reference while being compared against MERRA2 to account for uncertainties in the reanalysis products over the region.

4. Mechanisms Associated With AV

The objective of the present section is to assess the plausibility of *AV* deriving from the coupling. In particular, we aim to answer the following question: does the *AV* resulting from the coupling REMO-MPIOM (ROM) arise for the right reason? The term "right reason" here means that improved results in the mean climatology result from an improved representation of regional and local processes underlying the region's rainfall system.

4.1. Improvements in SSTs

The modulating role of SSTs on the equatorial African rainfall system is clearly established (Balas et al., 2007; Dezfuli & Nicholson, 2013; Nicholson & Dezfuli, 2013). Thus, we start our investigations by looking at how well the coupling is physically modifying prescribed SSTs from driving ESMs. It is crucial to acknowledge that ROM SST diverges from the ESM's SST, as it is influenced not only by external forcing but also by the coupled model's intrinsic dynamics. Particularly in regions where the ocean model's resolution significantly influences the representation of pertinent physical processes, substantial disparities between the two SSTs can emerge. Figure 4 displays REMO and ROM SST bias with regard to ERA5. It is noteworthy that in the atmospheric-only REMO simulations, the SST is directly inherited from ERA-Interim and MPI-ESM-LR, respectively. As a consequence, REMO-ERA features the smallest (slightly negative) SST bias over the Guinea Gulf (−0.32°C). The bias value approaches zero toward the interior of the Atlantic Ocean and southwards, including the South Atlantic High (SAH) pressure system. REMO-MPI-LR shows the highest positive SST bias (+1.93°C) over the whole Guinea Gulf and Benguela-Angola coastal seas. These positive biases propagate southwards along coastal areas and even over a large part of the SAH. The results of the coupled experiments argue for a systematic impact of ROM. In fact, the coupling leads to a positive SST bias (+0.89°C) in the ERA-Interim driven run (ROM-ERA). Similarly, the coupling considerably reduces the magnitudes of the positive SST bias (+0.45°C) as simulated by

21698996, 2024, 3, Downloaded from https://agupubs.onlinelibrary.wiley.com/doi/10.1029/2023JD039385 by Alfred Wegener Institut F. Polar- U. Meeresforschung Awi, Wiley Online Library on [30/10/2024]. See the Terms and Conditions (https://onlinelibrary.wiley.com/terms-and-conditions) on Wiley Online Library for rules of use; OA articles are governed by the applicable Creative Commons License

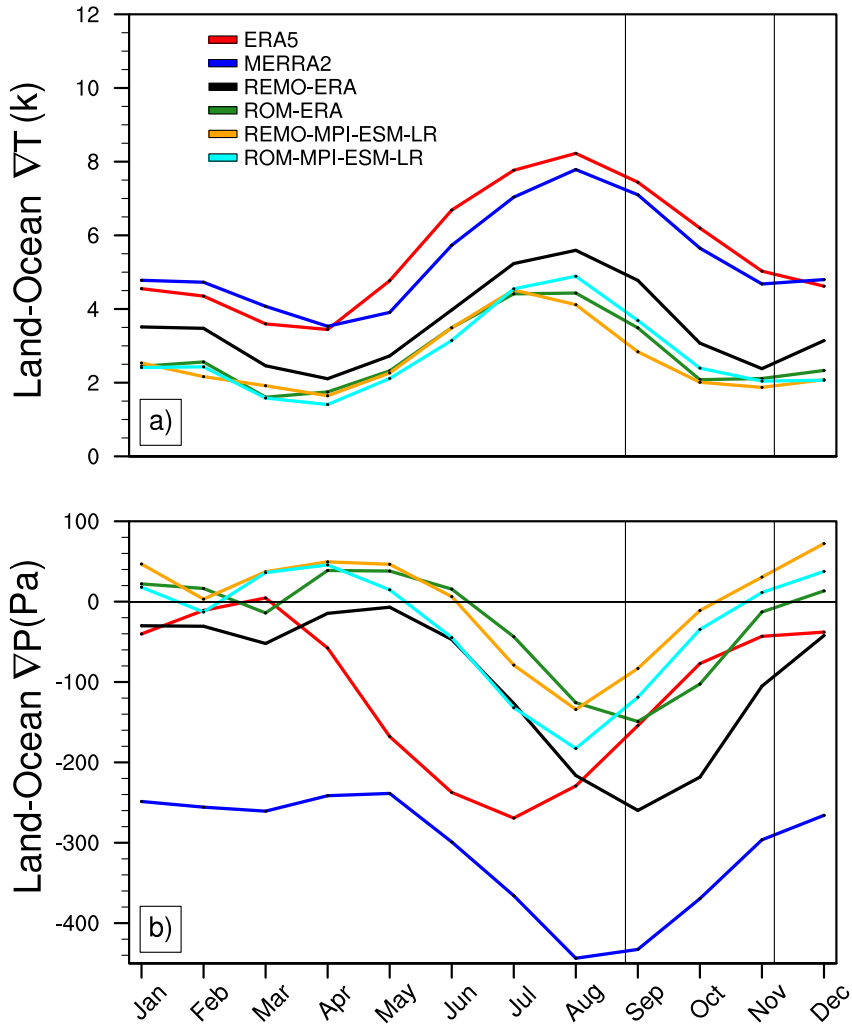

Figure 5. Mean (1980–2005) seasonality of the near-surface (a) land-ocean temperature difference (thermal contrast; ∇T in K) and (b) land-surface pressure and ocean sea-level pressure difference (∇P in Pa) between the interior of the continent (15°–30°E, 5°N–10°S) and the southeastern Atlantic Ocean (0°–10°E, 0°–10°S), for the reanalyzes ERA5 and MERRA2, and for REMO and ROM experiments. The lack bars delimit the SON season.

REMO-MPI-LR. In addition, the area of warm SST bias shifts southwards in the coupled simulations, giving way to cold biases in the coastal areas bordering West Africa. Similarly, the coupling considerably improves the representation of sea level pressures (SLP; Fig. S2 in Supporting Information S1), presumably in response to the improvement in SSTs.

Previous studies (e.g., Dyer et al., 2017; Pokam et al., 2012, 2014) demonstrated the role the Atlantic and Indian Oceans play in providing CEA with moisture. Modifications in SSTs due to coupling are expected to have substantial implications for the region's rainfall system. Indeed, an increase/decrease in SSTs (as simulated by ROM compared to REMO) suggests an increase/decrease in evaporation over the oceans feeding low-level westerlies (Pokam et al., 2014), southeasterlies (Dyer et al., 2017) and nocturnal low-level jets (Munday et al., 2021). Large- and mesoscale teleconnections might also be affected. For instance, modifications in SST in the Guinea Gulf influence the zonal temperature gradient (∇T), and the subsequent pressure contrast (∇P) between the landmass and the eastern equatorial Atlantic Ocean (Figure 5), with potential effect on the low- and mid-level circulation over the CEA. Specifically, Figure 5 shows that the reduction in warm SST bias over the eastern Atlantic Ocean results in a strengthening of the land-ocean thermal contrast (Figure 5a), enhancing the land-ocean pressure contrast (Figure 5b). Such changes led to variations in the strength of the atmospheric circulation and, consequently, in the amount of moisture advected into CEA and its penetration depth inland. Investigating how

21698996, 2024, 3, Downloaded from https://agupubs.onlinelibrary.wiley.com/doi/10.1029/2023JD039385 by Alfred Wegener Institut F. Polar- U. Meeresforschung Awi, Wiley Online Library on [30/10/2024]. See the Terms and Conditions (https://onlinelibrary.wiley.com/terms-and-conditions) on Wiley Online Library for rules of use; OA articles are governed by the applicable Creative Commons License

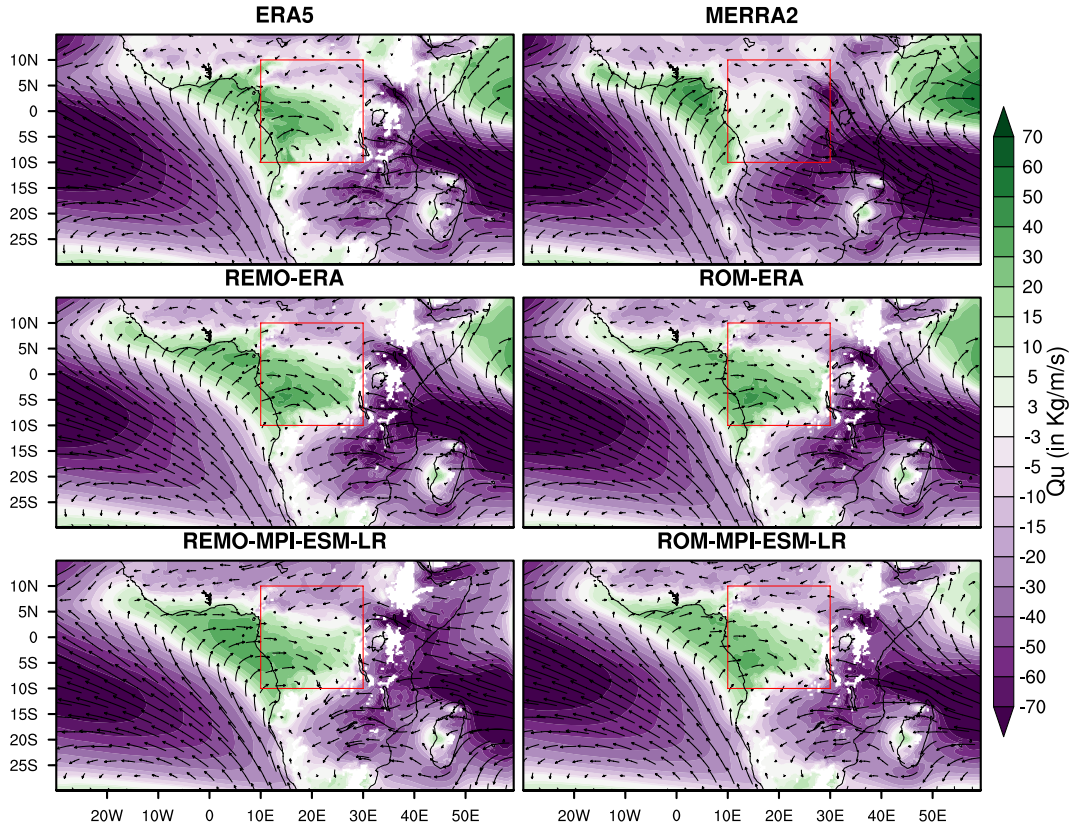

Figure 6. Mean (1980–2005) SON climatology of the lower layer (1,000–850 hPa) zonal vertically integrated moisture flux (Q_u, in Kg m^{-1} s^{-1}; shaded) superimposed with vertically integrated (1,000–850 hPa) total moisture transport (Q_T, in Kg m^{-1} s^{-1}; vectors), from the reanalysis datasets ERA5 and MERRA2, and from REMO and ROM experiments. Negative values indicate easterly flows and positive values are westerly flows. Red boxes denote the CEA.

the atmospheric circulation responds to changes in SSTs is thereby an important step in understanding the reasons for AV.

4.2. Improvements in the Atmospheric Circulation

We start looking at how the low-level circulation responds to modification in simulated SSTs and SLP. Figure 6 shows that both uncoupled and coupled simulations similarly distribute moisture fluxes in the lower layers of the troposphere, consistently with the ERA5 reanalysis. In fact, apart from MERRA2, the other datasets consistently show that the Atlantic Ocean supplies the CEA region with the largest fraction of mass flux via low-level westerlies. In addition, there is an agreement between the two experiments in the spatial pattern of the mass flux contribution from the East African Rift Valley System (Munday et al., 2021, 2023), together with advection from the southwestern Indian Ocean and from Sahelian regions.

The reason behind the patterns of *AV* shown in Figure 2 is further elucidated when quantifying the regional moisture convergence/divergence throughout the tropospheric column (Fig. S3 in Supporting Information S1). Indeed, REMO-ERA and ROM-ERA, which feature almost equal performance in modeling precipitation (Figure 3), also simulate a similar vertical profile of regional moisture convergence/divergence in the lower layers (1,000–850 hPa) and in all components (Fig. S3 in Supporting Information S1). Contrastingly, ROM-MPI-ESM-LR, which considerably improves the representation of precipitation climatology compared to its atmosphere-only counterpart REMO-MPI-ESM-LR, strongly reduces the magnitude of overestimated low-level inflows. The reduction of rainfall wet biases as modeled by ROM-MPI-ESM-LR is therefore associated with a weakening of the shallow moisture convergence driven by both the meridional component between 1,000 and 925 hPa (Fig. S3b in Supporting Information S1) and the zonal component up to 500 hPa (Fig. S3a in Supporting Information S1). This suggests that the coupling has a large influence on the representation of low-level westerlies as it strongly

21698996, 2024, 3, Downloaded from https://agupubs.onlinelibrary.wiley.com/doi/10.1029/2023JD039385 by Alfred Wegener Institut F. Polar- U. Meeresforschung Awi, Wiley Online Library on [30/10/2024]. See the Terms and Conditions (https://onlinelibrary.wiley.com/terms-and-conditions) on Wiley Online Library for rules of use; OA articles are governed by the applicable Creative Commons License

alters the land-ocean feedback in response to modification in SSTs and SLPs. This would result in a modification of land-ocean thermal and pressure contrasts.

The first implication of the modification of the low-level westerlies is the change in the longitudinal position and/or strength of the Congo Basin cell, a zonal shallow overturning and counterclockwise circulation over CEA (Longandjo & Rouault, 2020). In agreement with a previous study by Pokam et al. (2014), Longandjo and Rouault (2020) argued that, although this cell features a Walker-like circulation, it is isolated from the large-scale Atlantic-Indian Oceans Walker-type cells. The Congo basin cell is the response of the land-sea thermal and pressure contrasts between the CEA landmass and the eastern equatorial Atlantic Ocean. This cell is the engine of heat flux exchange between the warm CEA landmass and the cold eastern Atlantic Ocean through the establishment of a surface pressure gradient between the two regions which, in turn, triggers moisture transport into CEA through low-level westerlies (Pokam et al., 2014). Converging masses penetrate inland and disrupt atmospheric stability through increased moist static energy and topographic uplifts, thereby generating upward motions and, hence, convection. In simpler terms, moisture transported from the Congo Basin cell ascends through the upward branch of the Atlantic-Congo overturning circulation after uplift on the western side of the Rift Valley highlands. This moisture then enters the mesoscale convective systems (MCSs) embedded within the AEJs, which propagate westward, contributing to convection (Dezfuli et al., 2015). Tamoffo et al. (2022) showed that the atmosphere-only model simulates a weaker Congo basin cell compared to reanalyzes, resulting in less moisture advection inland and uneven spatial distribution. Figure 7 shows that REMO-ERA and ROM-ERA, which feature similar performance in simulating precipitation climatology (Figure 3a), also simulate a similar width, upward and eastward extension of the Cell. Furthermore, both experiments simulate almost equivalent cell intensity (Figure 8). However, a comparison between REMO-MPI-ESM-LR and ROM-MPI-ESM-LR reveals that the reduction in shallow mass convergence by the coupling is related to the increase in the strength of the Congo basin cell as well as to the rectification of its longitudinal positioning. Indeed, the coupling shifts the western edge of the cell eastward around 0° and limits its upward extension (Figure 7), which is more consistent with the ERA5 reanalysis, thus reducing the overestimated convective activity over the oceanic transect and western CEA. The eastward shift of the western edge of the cell is associated with a strengthening of the intensity of the cell (Figure 8). This, in turn, increases the amount of moisture transported from the west to the east of CEA, resulting in a more realistic distribution of moisture fluxes across the region.

In the middle layers (700–600 hPa) of the troposphere, the way in which the AEJs react to the coupling can also play an important role in the spatial pattern of the AV, since the AEJs strongly modulate the mid-tropospheric moisture transport (Pokam et al., 2012) and MCSs (Jackson et al., 2009). Indeed, Jackson et al. (2009) showed that during the rainiest season (SON), when both the northern (AEJ-N) and southern (AEJ-S) components of the jet are active, the mid-level moisture convergence into western equatorial Africa via the mid-layer easterlies reaches its maximum and it is stronger than the mid-level convergence during the March-April-May rainy season when only the AEJ-N is active. The presence of both jet components simultaneously favors a greater mass convergence in the mid-tropospheric layers, which increases the number of MCSs. This moisture advection feeds the upwards branch of the Atlantic-Congo circulation (Neupane, 2016) located west of the East African Rift Valley System (Dezfuli et al., 2015). Once again, REMO-ERA and ROM-ERA, which exhibited similar skills in reproducing precipitation climatology (Figure 3a), also display similar spatial patterns of moisture transport (Figure 9). However, the coupling induces slight changes in the intensity and the spatial extent of the area of AEJs' interaction. In fact, compared to REMO-ERA, ROM-ERA weakens the speed of easterlies over the southwestern CEA, thereby weakening the amount of outflows that could dry mid-layers and suppress the convection. When driven by the ESM, the coupled simulation (ROM-MPI-ESM-LR) succeeds in picking up the AEJ-S signal that is not detected by the atmosphere-only simulation REMO-MPI-ESM-LR (Figures 10b–10d). Likewise, the coupling shifts the AEJ-N's core northwards and enhances its intensity (Figure 11 and Figure S4 in Supporting Information S1). Compared to other datasets, including the ERA5 reanalysis, REMO-MPI-ESM-LR simulates an AEJ-N with an axis that is too inclined in the east-northwest direction, which is corrected in the ROM-MPI-ESM-LR simulation (Figures 9 and 11). Although the coupled and uncoupled simulations still merge the two jets compared to ERA5, the coupled runs separate the two jet cores more satisfactorily than the uncoupled ones (Figure 9 and Fig. S4 in Supporting Information S1). These results are consistent with previous findings on the AEJs-rainfall relationship over equatorial Africa. Jackson et al. (2009) showed that over western equatorial Africa, the enhanced AEJ-S is generally conducive to the increase in precipitation because of the response in the low-level mass inflows that strengthen at the right side of the jet entrance. This is correlated with the rainfall wet

21698996, 2024, 3, Downloaded from https://agupubs.onlinelibrary.wiley.com/doi/10.1029/2023JD039385 by Alfred Wegener Institut F. Polar- U. Meeresforschung Awi, Wiley Online Library on [30/10/2024]. See the Terms and Conditions (https://onlinelibrary.wiley.com/terms-and-conditions) on Wiley Online Library for rules of use; OA articles are governed by the applicable Creative Commons License

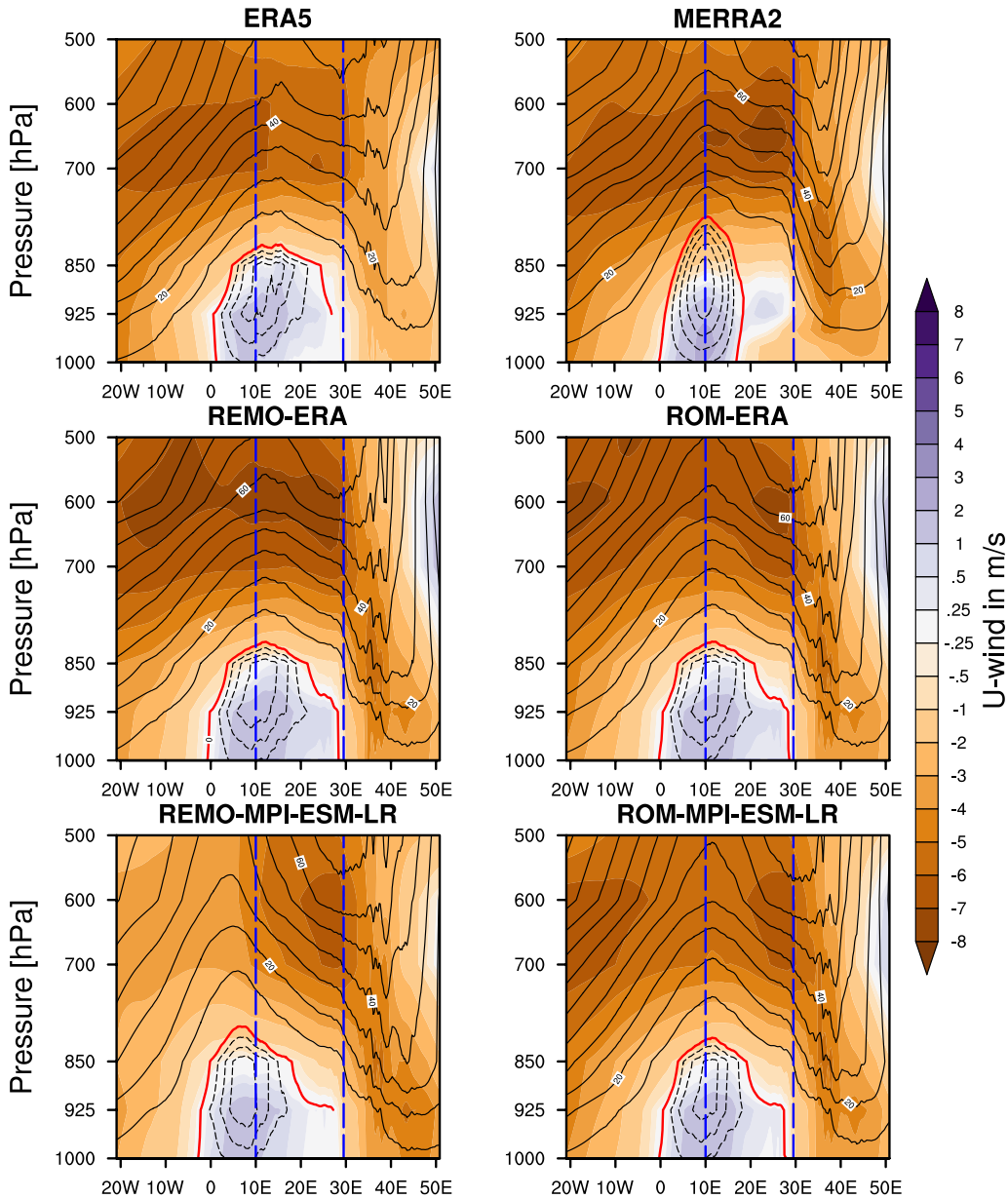

Figure 7. Mean (1980–2005) SON climatology of the zonal mass-weighted streamfunction (ψ_Z, contours in $10^{11} \times$ Kg s^{-1}) and mean zonal wind (shaded; in $m.s^{-1}$), from reanalysis data ERA5 and MERRA2, and from REMO and ROM experiments. Solid lines denote positive values of mass-weighted streamfunctions and dashed lines are negative values. The red line is the zero contour of the mass-weighted streamfunction ($\psi_Z = 0$) and delimits the Congo basin Cell. Contour intervals are -2×10^{11}Kg s^{-1} for negative values and 10×10^{11} Kg s^{-1} for positive values. The blue bars delimit the CEA.

bias simulated by the coupled run ROM-MPI-ESM-LR (Fig. S1 in Supporting Information S1). Similarly, the improvement in rainfall climatology as modeled by ROM-MPI-ESM-LR is a consequence of the improvement in the positioning (northwards shifting; Figure 10a and Figure S4 in Supporting Information S1) and intensity (increase; Figure 10c) of the AEJ-N (Dezfuli & Nicholson, 2013).

Finally, to ensure whether the coupling improves the representativeness of both jet components for the right reasons, we examined how the experiments simulate the precursor of the jets, specifically the surface meridional temperature gradient, as shown in Figure 12. Indeed, the AEJ-N results from the thermal gradient between the hot and dry Sahara and the moist Congo Basin, while the AEJ-S from that between the Kalahari and the Congo Basin. The AEJ-N (AEJ-S) develops along the southern (northern) edge of the maximum meridional surface temperature

21698996, 2024, 3, Downloaded from https://agupubs.onlinelibrary.wiley.com/doi/10.1029/2023JD039385 by Alfred Wegener Institut F. Polar- U. Meeresforschung Awi, Wiley Online Library on [30/10/2024]. See the Terms and Conditions (https://onlinelibrary.wiley.com/terms-and-conditions) on Wiley Online Library for rules of use; OA articles are governed by the applicable Creative Commons License

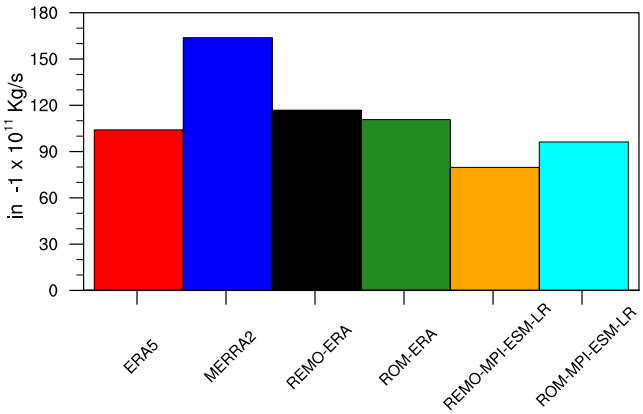

Figure 8. Mean (1980–2005) SON Congo basin cell (CBC) intensity (unit: -10^{11} Kg s^{-1}), from reanalysis data ERA5 and MERRA2, and from REMO and ROM experiments.

gradient, moving across latitudes throughout the year (specifically during the months of September-October–November). Figure 12 illustrates that improvements in the jets' representation are associated with enhancements in their underlying mechanisms. Indeed, the two reanalysis-forced runs (REMO-ERA and ROM-ERA) that demonstrate similar AEJ-N intensity over the 3 months (Figure 10c) also exhibit comparable gradient biases (Figures 12a and 12b). REMO-ERA simulates a stronger AEJ-S than ROM-ERA and even the ERA5 reanalysis, in association with its more pronounced negative gradient bias. When driven by the ESM, the coupled experiment ROM-MPI-ESM-LR significantly enhances both AEJ-N and AEJ-S intensities aligning with the ERA5 reanalysis) whereas the REMO-MPI-ESM-LR uncoupled simulation still underestimate them (Figures 10c and 10d). This improvement coincides with enhancements in the positive gradient (over the northern hemisphere) and negative gradient (over the southern hemisphere) that define the two jet components (Figures 12c and 12d).

5. Discussion and Conclusions

Realistically simulating the African climate system, particularly over CEA, remains challenging for the climate modeling community. One of the causes is the still incomplete understanding of the functioning of this region's climate system. For instance, the paucity of ground-based data made that region understudied with regards to neighboring areas such as West and South Africa in terms of analyzing the underlying processes and mechanisms, and therefore few works exist aimed

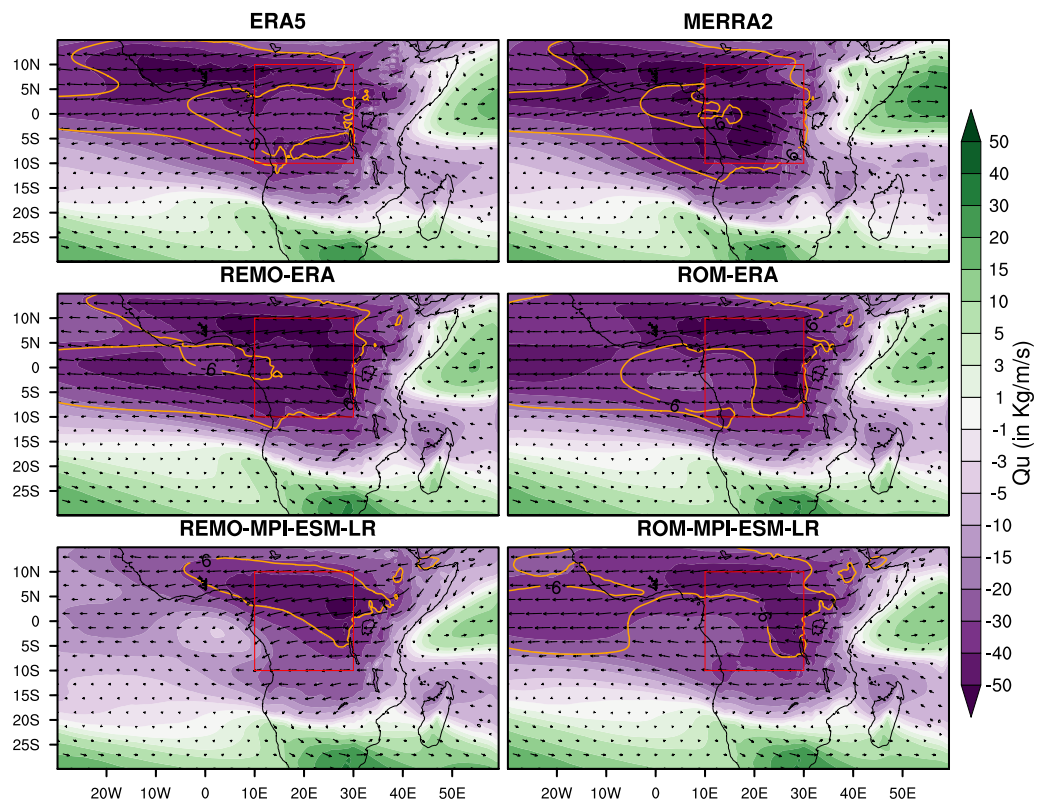

Figure 9. Mean (1980–2005) SON climatology of the middle layer (700-600 hPa) zonal vertically integrated moisture flux (Q_u, in Kg m^{-1} s^{-1}; shaded) superimposed with vertically integrated (700–600 hPa) total moisture transport (Q_T, in Kg m^{-1} s^{-1}; vectors), from the reanalysis datasets ERA5 and MERRA2, and from REMO and ROM experiments. The orange contours denote the area of interaction of AEJs. Negative values indicate easterly flows and positive values are westerly flows. Red boxes denote the CEA.

21698996, 2024, 3, Downloaded from https://agupubs.onlinelibrary.wiley.com/doi/10.1029/2023JD039385 by Alfred Wegener Institut F. Polar- U. Meeresforschung Awi, Wiley Online Library on [30/10/2024]. See the Terms and Conditions (https://onlinelibrary.wiley.com/terms-and-conditions) on Wiley Online Library for rules of use; OA articles are governed by the applicable Creative Commons License

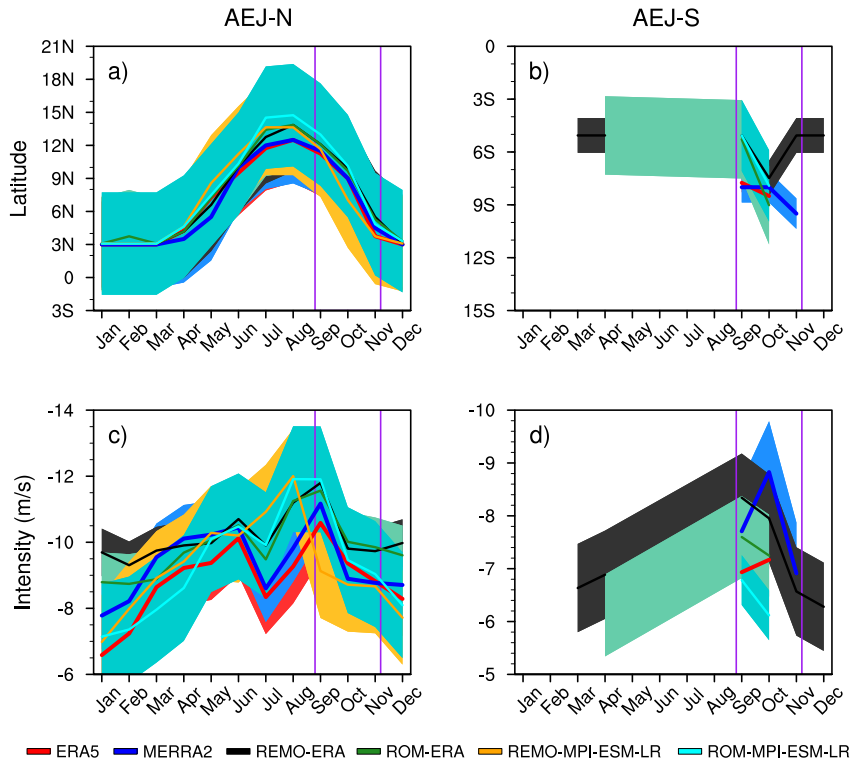

Figure 10. Mean (1980–2005) September–October–November intensity (in m/s; c–d) and location in (degrees latitudes; a–b) of monthly averages of the AEJ-N and AEJ-S jet cores in reanalysis data ERA5 and MERRA2, and in REMO and ROM experiments. The purple bars delimit the SON season. The corresponding shaded area in color represents the standard deviation, indicating the variability in both the jet location (a–b) and intensity (c–d).

at diagnosing the physical processes and mechanisms that underpin its rainfall system. So far, the problem of the scarcity of observational data remains over CEA (Nicholson et al., 2019; Washington et al., 2013). Climate models are helpful tools to deepen our knowledge of this region's climate system through sensitivity and test studies. Although Central Africa was not the primary focus of Coupled Model Intercomparison- and Coordinated Regional Climate Downscaling Experiment projects, numerous studies explored the climate of this region, capitalizing on the availability of climate models' data from these international programs. As aforementioned, despite substantial progress, not only both global and regional models still show large biases in the representation of past and present precipitation climatology (especially over equatorial Africa; Dosio, Jury, et al., 2021; Fotso-Kamga et al., 2020; Laprise et al., 2013; Nikulin et al., 2012; Panitz et al., 2014; Tamoffo, Vondou, et al., 2019, 2021,2022) but similar, if not larger, uncertainties also exist in the magnitude (and even sign) of the future precipitation change (e.g., Dosio, Jury, et al., 2021).

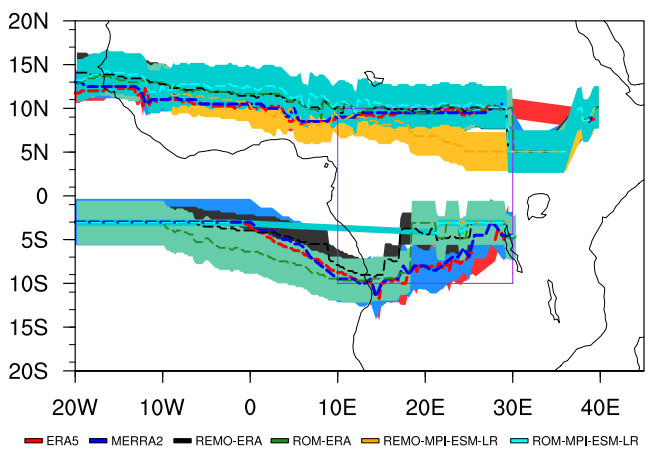

Figure 11. Long-term mean (1980–2005) SON latitudinal-longitudinal mean core locations of the AEJ-N (U-wind ≤ -6 m/s at 700 hPa in the northern hemisphere), and AEJ-S at 600 hPa in AEJ-S (U-wind ≤ -6 m/s at 600 hPa in the southern hemisphere); from reanalysis data ERA5 and MERRA2, and from REMO and ROM experiments. The purple box denotes CEA. The corresponding shaded area in color represents the standard deviation, indicating the variability in the jet location.

It is established that the dynamical downscaling by atmosphere-only models alone, although necessary (Munday et al., 2021), may be not sufficient to improve the representation of as complex climate systems as the African ones (Wu et al., 2020). The debate, therefore, focuses on the possibility of improving the models' skills not only by for example, increasing the horizontal resolution (which allows for better representation of small scale processes like convection; Stratton et al., 2018) but also by improving RCMs by coupling to additional components like interactive oceans, biogeochemistry, and aerosols

21698996, 2024, 3, Downloaded from https://agupubs.onlinelibrary.wiley.com/doi/10.1029/2023JD039385 by Alfred Wegener Institut F. Polar- U. Meeresforschung Awi, Wiley Online Library on [30/10/2024]. See the Terms and Conditions (https://onlinelibrary.wiley.com/terms-and-conditions) on Wiley Online Library for rules of use; OA articles are governed by the applicable Creative Commons License

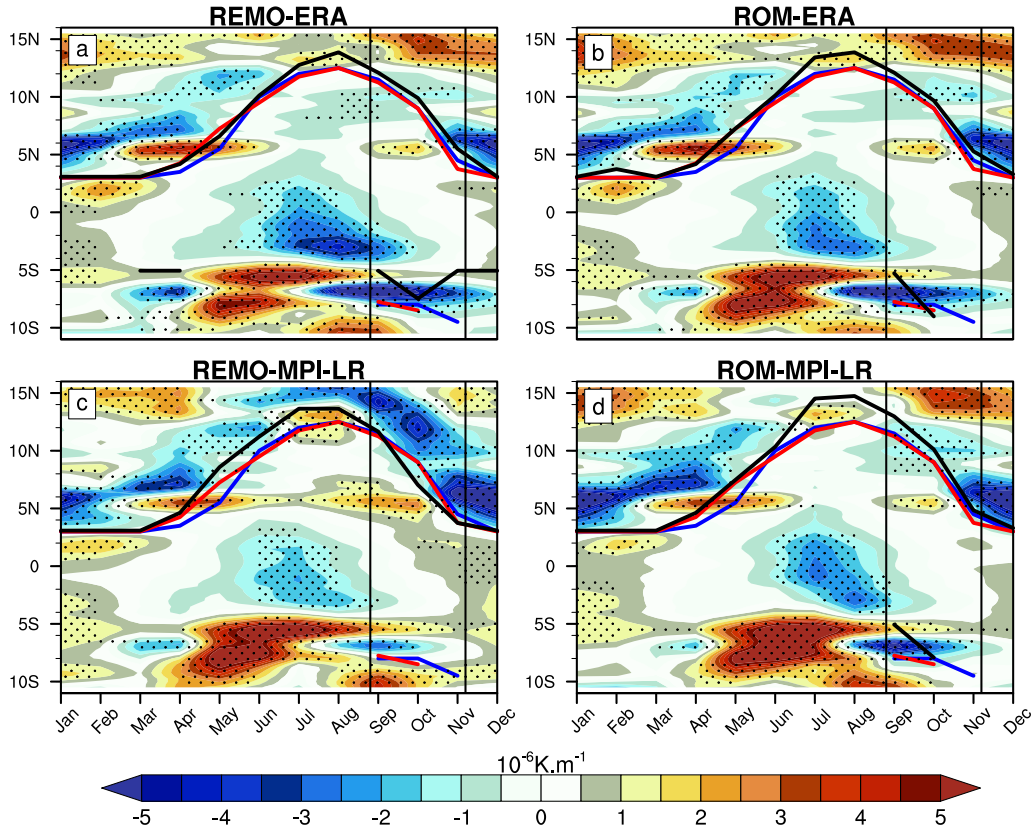

Figure 12. Long-term mean (1980–2005) climatology of the latitude/time annual cycle of the 850 hPa temperature gradient bias (10^{-6} K/m; REMO/ROM minus ERA5), averaged over the longitudes 14°–24°E. The black bars delimit the SON season. Contours in both hemispheres indicate the mean seasonal position of AEJs (i.e., u-wind > 6 m/s) from ERA5 (red), MERRA2 (blue) and the considered simulation (black). The stipples highlight the grid points where the gradient bias of the dataset under consideration is statistically significant at 95% confidence level using the Student's *t*-test. The black bars delimit the SON season.

(Doblas-Reyes et al., 2021). Wu et al. (2020) also demonstrated that improvements in spatial patterns of African rainfall biases generally required models' formulation.

Our results indeed show that the coupled atmosphere-ocean model ROM considerably reduces the positive SST bias as modelled by MPI-ESM-LR (bias that is, instead, inherited by the atmosphere-only model REMO) over the entire Guinea Gulf and Benguela-Angola coastal seas. This results in a better representation of low-level westerlies and the Congo basin cell, and thus of the precipitation climatology. The enhancement of the Congo basin cell also presumably implies a better representation of the large-scale Atlantic-Congo zonal overturning circulation (Neupane, 2016; Pokam et al., 2014) and, subsequently, of land-ocean thermal and pressure contrasts in coupled experiments: as the zonal overturning circulation is modulated by SST, coupled general circulation models generally represent it more realistically than their atmosphere-only counterpart, as demonstrated for CEA by Taguela et al. (2022). We also found that in the mid-tropospheric layers, the coupling improves the representation of the intensity and spatial extent of AEJs. The better representation of SSTs improves the surface meridional thermal gradients that setup AEJs (Nicholson & Grist, 2003), and their maintenance mechanisms (Chen, 2005; Kuete et al., 2019).

The present study also demonstrates that dynamical downscaling by means of a coupled global ocean-regional atmosphere model plausibly improves the representation of the CEA climate system with respect to the result of an atmosphere-only RCM. In particular, coupled experiments add value compared to their corresponding uncoupled experiments (also see Weber et al., 2022), especially when forced by ESMs (MPI-ESM-LR ESM used in the present study) as opposed to reanalysis. Although the robustness of our results needs to be assessed by extending it to other driving ESMs, our work suggests the benefit of using coupled RCMs to downscale ESM results also

21698996, 2024, 3, Downloaded from https://agupubs.onlinelibrary.wiley.com/doi/10.1029/2023JD039385 by Alfred Wegener Institut F. Polar- U. Meeresforschung Awi, Wiley Online Library on [30/10/2024]. See the Terms and Conditions (https://onlinelibrary.wiley.com/terms-and-conditions) on Wiley Online Library for rules of use; OA articles are governed by the applicable Creative Commons License

21698996, 2024, 3, Downloaded from https://agupubs.onlinelibrary.wiley.com/doi/10.1029/2023JD039385 by Alfred Wegener Institut F. Polar- U. Meeresforschung Awi, Wiley Online Library on [30/10/2024]. See the Terms and Conditions (https://onlinelibrary.wiley.com/terms-and-conditions) on Wiley Online Library for rules of use; OA articles are governed by the applicable Creative Commons License

for future climate projections. However, there is evidence that regionally coupled atmosphere-ocean models such as ROM, although promising, still require improvements as also noted by Sein et al. (2015). In fact, the atmospheric component of ROM still makes use of parameterized convection, which is nowadays found unsuitable for modelling the equatorial African rainfall system. The parameterised convection usually associated intense convection (strong ascent motions) with the heaviest rainfall events. However, this is not the case in equatorial Africa (Hamada et al., 2015), or at least in CEA. A number of studies (e.g., Alber et al., 2021; Raghavendra et al., 2018) showed that despite the increasing trend in thunderstorms over the Congo basin, the rainfall trend is contrastingly decreasing, leading to a drying of the Congo rainforest. Convection-permitting modelling (CPM) is a promising approach to simulating precipitation features across Africa because it connects better deep convection and precipitation variability (Lucas-Picher et al., 2021). The CPMs considerably improve the rainfall features such as the intensity and diurnal cycle, together with the large-scale atmospheric circulation (Senior et al., 2021). Unfortunately, the high cost of computational resources that requires the CPM makes its usage still limited. However, based on the promising results using CPMs and regional coupled atmosphere-ocean models over CEA, the development of a regional coupled atmosphere-ocean CPM should be envisaged.

Finally, it must be noted that the atmospheric circulation patterns can be influenced by other mechanisms besides those investigated in this study, such as, for instance, the surface energy budget. Although a preliminary analysis (not shown) seems to confirm that the energy budget is not directly influenced by the coupling, a thorough investigation of the role of the different components of the heat fluxes and their distribution within the atmosphere could provide insights into the vertical transport of energy and its impact on atmospheric circulation. This is left for future research.

Conflict of Interest

The authors declare no conflicts of interest relevant to this study.

Data Availability Statement

The model simulations were performed at the German Climate Computing Center (Deutsches Klimarechenzentrum, DKRZ) in Hamburg. All observational and reanalysis data used in this study are publicly available at no charge and with unrestricted access. The ERA5/ERA-Interim reanalysis datasets are publicly available from the Copernicus Climate Change Service (C3S) Climate Data Store (CDS) at (Hersbach et al., 2020/Dee et al., 2011) https://cds.climate.copernicus.eu/cdsapp#!/dataset/reanalysis-era5-pressure-levels-monthly-means?tab1/4form. The MERRA-2 dataset can be downloaded from the Global Modeling and Assimilation Office at (NASA, 2016) https://disc.gsfc.nasa.gov/datasets?keywords1/4%22MERRA-2%22&page1/41&source1/4Models%2FAnalyses%20MERRA-2. The GPCC observational dataset is available at (Schneider et al., 2022) https://opendata.dwd.de/climate_environment/GPCC/html/fulldata-monthly_v2020_doi_download.html. The CRU-v4.04 dataset is available at (Harris et al., 2020) https://data.ceda.ac.uk/badc/cru/data/cru_ts/cru_ts_4.05/data/pre. The CHIRPS2 dataset are available at (Funk et al., 2015) https://data.chc.ucsb.edu/products/CHIRPS-2.0/global_daily/netcdf/.

Acknowledgments
The first author is funded by the Humboldt-Stiftung as part of the Humboldt Research Fellowship for researchers of all nationalities and research areas: postdoctoral and experienced researchers programme. Open access funding is provided by Helmholtz-Zentrum Hereon. We thank the Climate Service Center (GERICS) for performing atmospheric-only REMO and coupled ROM simulations. D. V. Sein received funding from the Federal Ministry of Education and Research of Germany (BMBF) in the framework of ACE project (Grant 01LP2004A) and the Ministry of Science and Higher Education of Russia (theme no. FMWE-2021-0014). William Cabos has been funded by the Alcala University project PIUAH21/CC-058 and the Spanish Ministry of Science, Innovation and Universities, through grant (PID2021-128656OB-I00). Furthermore, the authors would like to thank the German Climate Computing Center (DKRZ) in Hamburg for providing the high-computing capacity. Thank you to all the reanalysis, satellite and observational data providers used in this study. The helpful input of Lars Buntemeyer was also really appreciated. The authors thank the two anonymous reviewers and the editor whose comments helped improve and clarify this manuscript. Open Access funding enabled and organized by Projekt DEAL.

References

Alber, K., Raghavendra, A., Zhou, L., Jiang, Y., Sussman, H. S., & Solimine, S. L. (2021). Analyzing intensifying thunderstorms over the Congo Basin using the Gálvez-Davison index from 1983–2018. *Climate Dynamics*, *56*(3–4), 949–967. https://doi.org/10.1007/s00382-020-05513-x

Balas, N., Nicholson, S. E., & Klotter, D. (2007). The relationship of rainfall variability in West Central Africa to sea-surface temperature fluctuations. *International Journal of Climatology*, *27*(10), 1335–1349. https://doi.org/10.1002/joc.1456

Cabos, W., Sein, D., De La Vara, A., & Alvarez Garcia, F. (2020). *Impact of ocean-atmosphere coupling on regional climate: The Iberian Peninsula case*. Copernicus GmbH. https://doi.org/10.5194/egusphere-egu2020-13098

Chen, T.-C. (2005). Maintenance of the midtropospheric north African summer circulation: Saharan high and African easterly jet. *Journal of Climate*, *18*(15), 2943–2962. https://doi.org/10.1175/jcli3446.1

Creese, A., & Washington, R. (2018). A process-based assessment of CMIP5 rainfall in the Congo basin: The September–November rainy season. *Journal of Climate*, *31*(18), 7417–7439. https://doi.org/10.1175/jcli-d-17-0818.1

Crétat, J., Vizy, E. K., & Cook, K. H. (2013). How well are daily intense rainfall events captured by current climate models over Africa? *Climate Dynamics*, *42*(9–10), 2691–2711. https://doi.org/10.1007/s00382-013-1796-7

Dee, D. P., Uppala, S. M., Simmons, A. J., Berrisford, P., Poli, P., Kobayashi, S., et al. (2011). The ERA-Interim reanalysis: Configuration and performance of the data assimilation system [Dataset]. Quarterly Journal of the Royal Meteorological Society, *137*(656), 553–597. https://doi.org/10.1002/qj.828

Dezfuli, A. K., & Nicholson, S. E. (2013). The relationship of rainfall variability in western equatorial Africa to the tropical oceans and atmospheric circulation. Part II: The boreal autumn. *Journal of Climate*, *26*(1), 66–84. https://doi.org/10.1175/jcli-d-11-00686.1

Dezfuli, A. K., Zaitchik, B. F., & Gnanadesikan, A. (2015). Regional atmospheric circulation and rainfall variability in south equatorial Africa. *Journal of Climate*, *28*(2), 809–818. https://doi.org/10.1175/jcli-d-14-00333.1

Di Luca, A., Elía, R. D., & Laprise, R. (2012). Potential for small scale added value of RCM's downscaled climate change signal. *Climate Dynamics*, *40*(3–4), 601–618. https://doi.org/10.1007/s00382-012-1415-z

Doblas-Reyes, F. J., Sörensson, A. A., Almazroui, M., Dosio, A., Gutowski, W. J., Haarsma, R., et al. (2021). Linking global to regional climate change. In V. Masson-Delmotte, P. Zhai, A. Pirani, S. L. Connors, C. Péan, S. Berger, et al. (Eds.), *Climate change 2021: The physical science basis. Contribution of working group I to the sixth assessment report of the intergovernmental Panel on climate change [* (pp. 1363–1512). Cambridge University Press. https://doi.org/10.1017/9781009157896.012

Dosio, A., Jones, R. G., Jack, C., Lennard, C., Nikulin, G., & Hewitson, B. (2019). What can we know about future precipitation in Africa? Robustness, significance and added value of projections from a large ensemble of regional climate models. *Climate Dynamics*, *53*(9–10), 5833–5858. https://doi.org/10.1007/s00382-019-04900-3

Dosio, A., Jury, M. W., Almazroui, M., Ashfaq, M., Diallo, I., Engelbrecht, F. A., et al. (2021). Projected future daily characteristics of African precipitation based on global (CMIP5, CMIP6) and regional (CORDEX, CORDEX-CORE) climate models. *Climate Dynamics*, *57*(11–12), 3135–3158. https://doi.org/10.1007/s00382-021-05859-w

Dosio, A., & Panitz, H.-J. (2015). Climate change projections for CORDEX-Africa with COSMO-CLM regional climate model and differences with the driving global climate models. *Climate Dynamics*, *46*(5–6), 1599–1625. https://doi.org/10.1007/s00382-015-2664-4

Dosio, A., Panitz, H.-J., Schubert-Frisius, M., & Lüthi, D. (2015). Dynamical downscaling of CMIP5 global circulation models over CORDEX-Africa with COSMO-CLM: Evaluation over the present climate and analysis of the added value. *Climate Dynamics*, *44*(9–10), 2637–2661. https://doi.org/10.1007/s00382-014-2262-x

Dosio, A., Pinto, I., Lennard, C., Sylla, M. B., Jack, C., & Nikulin, G. (2021). What can we know about recent past precipitation over Africa? Daily characteristics of African precipitation from a large ensemble of observational products for model evaluation. *Earth and Space Science*, *8*(10). https://doi.org/10.1029/2020ea001466

Dyer, E. L. E., Jones, D. B. A., Nusbaumer, J., Li, H., Collins, O., Vettoretti, G., & Noone, D. (2017). Congo Basin precipitation: Assessing seasonality, regional interactions, and sources of moisture. *Journal of Geophysical Research: Atmospheres*, *122*(13), 6882–6898. https://doi.org/10.1002/2016jd026240

Fotso-Kamga, G., Fotso-Nguemo, T. C., Diallo, I., Yepdo, Z. D., Pokam, W. M., Vondou, D. A., & Lenouo, A. (2020). An evaluation of COSMO-CLM regional climate model in simulating precipitation over Central Africa. *International Journal of Climatology*, *40*(5), 2891–2912. https://doi.org/10.1002/joc.6372

Fotso-Nguemo, T. C., Diallo, I., Diakhaté, M., Vondou, D. A., Mbaye, M. L., Haensler, A., et al. (2019). Projected changes in the seasonal cycle of extreme rainfall events from CORDEX simulations over Central Africa. *Climatic Change*, *155*(3), 339–357. https://doi.org/10.1007/s10584-019-02492-9

Fotso-Nguemo, T. C., Vondou, D. A., Tchawoua, C., & Haensler, A. (2016). Assessment of simulated rainfall and temperature from the regional climate model REMO and future changes over Central Africa. *Climate Dynamics*, *48*(11–12), 3685–3705. https://doi.org/10.1007/s00382-016-3294-1

Funk, C., Peterson, P., Landsfeld, M., Pedreros, D., Verdin, J., Shukla, S., et al. (2015). "The climate hazards infrared precipitation with stations—A new environmental record for monitoring extremes" [dataset]. Scientific Data, *2*, 150066–150071. https://doi.org/10.1038/sdata.2015.66

Gibba, P., Sylla, M. B., Okogbue, E. C., Gaye, A. T., Nikiema, M., & Kebe, I. (2018). State-of-the-art climate modeling of extreme precipitation over Africa: Analysis of CORDEX added-value over CMIP5. *Theoretical and Applied Climatology*, *137*(1–2), 1041–1057. https://doi.org/10.1007/s00704-018-2650-y

Giorgi, F., & Gutowski, W. J., Jr. (2015). Regional dynamical downscaling and the CORDEX initiative. *Annual Review of Environment and Resources*, *40*(1), 467–490. https://doi.org/10.1146/annurev-environ-102014-021217

Haensler, A., Hagemann, S., & Jacob, D. (2011). The role of the simulation setup in a long-term high-resolution climate change projection for the southern African region. *Theoretical and Applied Climatology*, *106*(1–2), 153–169. https://doi.org/10.1007/s00704-011-0420-1

Haensler, A., Saeed, F., & Jacob, D. (2013). Assessing the robustness of projected precipitation changes over central Africa on the basis of a multitude of global and regional climate projections. *Climatic Change*, *121*(2), 349–363. https://doi.org/10.1007/s10584-013-0863-8

Hamada, A., Takayabu, Y. N., Liu, C., & Zipser, E. J. (2015). Weak linkage between the heaviest rainfall and tallest storms. *Nature Communications*, *6*(1), 6213. https://doi.org/10.1038/ncomms7213

Harris, I., Osborn, T. J., Jones, P., & Lister, D. (2020). Version 4 of the CRU TS monthly high-resolution gridded multivariate climate dataset [Dataset]. Scientific Data, *7*(1), 109. https://doi.org/10.1038/s41597-020-0453-3

Hernández-Díaz, L., Laprise, R., Nikiéma, O., & Winger, K. (2016). 3-Step dynamical downscaling with empirical correction of sea-surface conditions: Application to a CORDEX Africa simulation. *Climate Dynamics*, *48*(7–8), 2215–2233. https://doi.org/10.1007/s00382-016-3201-9

Hersbach, H., Bell, B., Berrisford, P., Hirahara, S., Horányi, A., Muñoz-Sabater, J., et al. (2020). The ERA5 global reanalysis [Dataset]. Quarterly Journal of the Royal Meteorological Society, *146*(730), 1999–2049. https://doi.org/10.1002/qj.3803

Hoffmann, P., Katzfey, J. J., McGregor, J. L., & Thatcher, M. (2016). Bias and variance correction of sea surface temperatures used for dynamical downscaling. *Journal of Geophysical Research: Atmospheres*, *121*(21), 12877–12890. https://doi.org/10.1002/2016jd025383

Jackson, B., Nicholson, S. E., & Klotter, D. (2009). Mesoscale convective systems over Western Equatorial Africa and their relationship to large-scale circulation. *Monthly Weather Review*, *137*(4), 1272–1294. https://doi.org/10.1175/2008mwr2525.1

Jacob, D. (2001). The role of water vapour in the atmosphere. A short overview from a climate modeller's point of view. *Physics and Chemistry of the Earth*, *26*(6–8), 523–527. https://doi.org/10.1016/s1464-1895(01)00094-1

Jacob, D., Elizalde, A., Haensler, A., Hagemann, S., Kumar, P., Podzun, R., et al. (2012). Assessing the transferability of the regional climate model REMO to different coordinated regional climate downscaling experiment (CORDEX) regions. *Atmosphere*, *3*(1), 181–199. https://doi.org/10.3390/atmos3010181

James, R., Washington, R., Abiodun, B., Kay, G., Mutemi, J., Pokam, W., et al. (2017). Evaluating climate models with an African lens. *Bulletin of the American Meteorological Society*, *99*(2), 313–336. https://doi.org/10.1175/bams-d-16-0090.1

Jungclaus, J. H., Fischer, N., Haak, H., Lohmann, K., Marotzke, J., Matei, D., et al. (2013). Characteristics of the ocean simulations in the Max Planck Institute Ocean Model (MPIOM) the ocean component of the MPI-earth system model. *Journal of Advances in Modeling Earth Systems*, *5*(2), 422–446. https://doi.org/10.1002/jame.20023

Kuete, G., Mba, W. P., James, R., Dyer, E., Annor, T., & Washington, R. (2022). How do coupled models represent the African Easterly Jets and their associated dynamics over Central Africa during the September–November rainy season? *Climate Dynamics*, *60*(9–10), 2907–2929. https://doi.org/10.1007/s00382-022-06467-y

21698996, 2024, 3, Downloaded from https://agupubs.onlinelibrary.wiley.com/doi/10.1029/2023JD039385 by Alfred Wegener Institut F. Polar- U. Meeresforschung Awi, Wiley Online Library on [30/10/2024]. See the Terms and Conditions (https://onlinelibrary.wiley.com/terms-and-conditions) on Wiley Online Library for rules of use; OA articles are governed by the applicable Creative Commons License

Kuete, G., Pokam Mba, W., & Washington, R. (2019). African easterly jet south: Control, maintenance mechanisms and link with southern subtropical waves. *Climate Dynamics*, *54*(3–4), 1539–1552. https://doi.org/10.1007/s00382-019-05072-w

Laprise, R., Hernández-Díaz, L., Tete, K., Sushama, L., Šeparović, L., Martynov, A., et al. (2013). Climate projections over CORDEX Africa domain using the fifth-generation Canadian regional climate model (CRCM5). *Climate Dynamics*, *41*(11–12), 3219–3246. https://doi.org/10.1007/s00382-012-1651-2

Longandjo, G. N. T., & Rouault, M. (2020). On the structure of the regional-scale circulation over central Africa: Seasonal evolution, variability, and mechanisms. *Journal of Climate*, *33*(1), 145–162. https://doi.org/10.1175/JCLI-D-19-0176.1

Lucas-Picher, P., Argüeso, D., Brisson, E., Tramblay, Y., Berg, P., Lemonsu, A., et al. (2021). Convection-permitting modeling with regional climate models: Latest developments and next steps. *WIREs Climate Change*, *12*(6). https://doi.org/10.1002/wcc.731

Munday, C., Savage, N., Jones, R. G., & Washington, R. (2023). Valley formation aridifies East Africa and elevates Congo Basin rainfall. *Nature*, *615*(7951), 276–279. https://doi.org/10.1038/s41586-022-05662-5

Munday, C., Washington, R., & Hart, N. (2021). African low-level jets and their importance for water vapor transport and rainfall. *Geophysical Research Letters*, *48*(1). https://doi.org/10.1029/2020gl090999

NASA. (2016). Modern-era retrospective analysis for research and applications, version 2 (MERRA2). Goddard Earth Sciences Data and Information Services Center. Retrieved from https://disc.gsfc.nasa.gov/daac-bin/FTPSubset.pl. accessed 12 September 2017 [Dataset]

Neupane, N. (2016). The Congo basin zonal overturning circulation. *Advances in Atmospheric Sciences*, *33*(6), 767–782. https://doi.org/10.1007/s00376-015-5190-8

Nicholson, S. E., & Dezfuli, A. K. (2013). The relationship of rainfall variability in western equatorial Africa to the tropical oceans and atmospheric circulation. Part I: The boreal spring. *Journal of Climate*, *26*(1), 45–65. https://doi.org/10.1175/jcli-d-11-00653.1

Nicholson, S. E., & Grist, J. P. (2003). The seasonal evolution of the atmospheric circulation over West Africa and equatorial Africa. *Journal of Climate*, *16*(7), 1013–1030. https://doi.org/10.1175/1520-0442(2003)016<1013:tseota>2.0.co;2

Nicholson, S. E., Klotter, D., Zhou, L., & Hua, W. (2019). Validation of satellite precipitation estimates over the Congo Basin. *Journal of Hydrometeorology*, *20*(4), 631–656. https://doi.org/10.1175/jhm-d-18-0118.1

Nikulin, G., Jones, C., Giorgi, F., Asrar, G., Büchner, M., Cerezo-Mota, R., et al. (2012). Precipitation climatology in an ensemble of cordex-Africa regional climate simulations. *Journal of Climate*, *25*(18), 6057–6078. https://doi.org/10.1175/jcli-d-11-00375.1

Panitz, H.-J., Dosio, A., Büchner, M., Lüthi, D., & Keuler, K. (2014). COSMO-CLM (CCLM) climate simulations over CORDEX-Africa domain: Analysis of the ERA-Interim driven simulations at 0.44° and 0.22° resolution. *Climate Dynamics*, *42*(11–12), 3015–3038. https://doi.org/10.1007/s00382-013-1834-5

Paxian, A., Sein, D., Panitz, H.-J., Warscher, M., Breil, M., Engel, T., et al. (2016). Bias reduction in decadal predictions of West African monsoon rainfall using regional climate models. *Journal of Geophysical Research: Atmospheres*, *121*(4), 1715–1735. https://doi.org/10.1002/2015jd024143

Pokam, W., Bain, C. L., Chadwick, R. S., Graham, R., Sonwa, D. J., & Kamga, F. M. (2014). Identification of processes driving low-level westerlies in west equatorial Africa. *Journal of Climate*, *27*(11), 4245–4262. https://doi.org/10.1175/JCLI-D-13-00490.1

Pokam, W. M., Djiotang, L. A. T., & Mkankam, F. K. (2012). Atmospheric water vapor transport and recycling in Equatorial Central Africa through NCEP/NCAR reanalysis data. *Climate Dynamics*, *38*(9–10), 1715–1729. https://doi.org/10.1007/s00382-011-1242-7

Raghavendra, A., Zhou, L., Jiang, Y., & Hua, W. (2018). Increasing extent and intensity of thunderstorms observed over the Congo Basin from 1982 to 2016. *Atmospheric Research*, *213*, 17–26. https://doi.org/10.1016/j.atmosres.2018.05.028

Ratnam, J. V., Morioka, Y., Behera, S. K., & Yamagata, T. (2015). A model study of regional air-sea interaction in the austral summer precipitation over southern Africa. *Journal of Geophysical Research: Atmospheres*, *120*(6), 2342–2357. https://doi.org/10.1002/2014jd022154

Samanta, D., Hameed, S. N., Jin, D., Thilakan, V., Ganai, M., Rao, S. A., & Deshpande, M. (2018). Impact of a narrow Coastal Bay of Bengal Sea surface temperature front on an indian summer monsoon simulation. *Scientific Reports*, *8*(1), 17694. https://doi.org/10.1038/s41598-018-35735-3

Schneider, U., Hänsel, S., Finger, P., Rustemeier, E., & Ziese, M. (2022). GPCC full data monthly product version 2022 at 0.25°: Monthly land-surface precipitation from rain-gauges built on GTS-based and historical data. [Dataset]. https://doi.org/10.5676/DWD_GPCC/FD_M_V2022_025

Sein, D. V., Koldunov, N. V., Pinto, J. G., & Cabos, W. (2014). Sensitivity of simulated regional Arctic climate to the choice of coupled model domain. *Tellus A: Dynamic Meteorology and Oceanography*, *66*(1), 23966. https://doi.org/10.3402/tellusa.v66.23966

Sein, D. V., Mikolajewicz, U., Gröger, M., Fast, I., Cabos, W., Pinto, J. G., et al. (2015). Regionally coupled atmosphere-ocean-sea ice-marine biogeochemistry model ROM: 1. Description and validation. *Journal of Advances in Modeling Earth Systems*, *7*(1), 268–304. https://doi.org/10.1002/2014ms000357

Senior, C. A., Marsham, J. H., Berthou, S., Burgin, L. E., Folwell, S. S., Kendon, E. J., et al. (2021). Convection-permitting regional climate change simulations for understanding future climate and informing decision-making in Africa. *Bulletin of the American Meteorological Society*, *102*(6), E1206–E1223. https://doi.org/10.1175/bams-d-20-0020.1

Sørland, S. L., Brogli, R., Pothapakula, P. K., Russo, E., Van De Walle, J., Ahrens, B., et al. (2021). Cosmo-clm regional climate simulations in the cordex framework: A review. *Climate Earth System Modelling*. https://doi.org/10.5194/gmd-2020-443

Stevens, B., Giorgetta, M., Esch, M., Mauritsen, T., Crueger, T., Rast, S., et al. (2013). Atmospheric component of the MPI-M earth system model: ECHAM6. *Journal of Advances in Modeling Earth Systems*, *5*(2), 146–172. https://doi.org/10.1002/jame.20015

Stratton, R. A., Senior, C. A., Vosper, S. B., Folwell, S. S., Boutle, I. A., Earnshaw, P. D., et al. (2018). A Pan-African convection-permitting regional climate simulation with the Met Office unified model: CP4-Africa. *Journal of Climate*, *31*(9), 3485–3508. https://doi.org/10.1175/jcli-d-17-0503.1

Sylla, M. B., Giorgi, F., Coppola, E., & Mariotti, L. (2012). Uncertainties in daily rainfall over Africa: Assessment of gridded observation products and evaluation of a regional climate model simulation. *International Journal of Climatology*, *33*(7), 1805–1817. https://doi.org/10.1002/joc.3551

Taguela, T. N., Pokam, W. M., & Washington, R. (2022). Rainfall in uncoupled and coupled versions of the Met Office unified model over central Africa: Investigation of processes during the September–November rainy season. *International Journal of Climatology*, *42*(12), 6311–6331. https://doi.org/10.1002/joc.7591

Taguela, T. N., Vondou, D. A., Moufouma-Okia, W., Fotso-Nguemo, T. C., Pokam, W. M., Tanessong, R. S., et al. (2020). CORDEX multi-rcm hindcast over central Africa: Evaluation within observational uncertainty. *Journal of Geophysical Research: Atmospheres*, *125*(5). https://doi.org/10.1029/2019jd031607

Tamoffo, A. T., Amekudzi, L. K., Weber, T., Vondou, D. A., Yamba, E. I., & Jacob, D. (2022). Mechanisms of rainfall biases in two CORDEX-CORE regional climate models at rainfall peaks over central equatorial Africa. *Journal of Climate*, *35*(2), 639–668. https://doi.org/10.1175/jcli-d-21-0487.1

21698996, 2024, 3, Downloaded from https://agupubs.onlinelibrary.wiley.com/doi/10.1029/2023JD039385 by Alfred Wegener Institut F. Polar- U. Meeresforschung Awi, Wiley Online Library on [30/10/2024]. See the Terms and Conditions (https://onlinelibrary.wiley.com/terms-and-conditions) on Wiley Online Library for rules of use; OA articles are governed by the applicable Creative Commons License

Tamoffo, A. T., Dosio, A., Vondou, D. A., & Sonkoué, D. (2020). Process-Based analysis of the added value of dynamical downscaling over central Africa. *Geophysical Research Letters*, *47*(17). https://doi.org/10.1029/2020gl089702

Tamoffo, A. T., Moufouma-Okia, W., Dosio, A., James, R., Pokam, W. M., Vondou, D. A., et al. (2019). Process-oriented assessment of RCA4 regional climate model projections over the Congo Basin under 1.5°C and 2°C global warming levels: Influence of regional moisture fluxes. *Climate Dynamics*, *53*(3–4), 1911–1935. https://doi.org/10.1007/s00382-019-04751-y

Tamoffo, A. T., Nikulin, G., Vondou, D. A., Dosio, A., Nouayou, R., Wu, M., & Igri, P. M. (2021). Process-based assessment of the impact of reduced turbulent mixing on Congo Basin precipitation in the RCA4 Regional Climate Model. *Climate Dynamics*, *56*(5–6), 1951–1965. https://doi.org/10.1007/s00382-020-05571-1

Tamoffo, A. T., Vondou, D. A., Pokam, W. M., Haensler, A., Yepdo, Z. D., Fotso-Nguemo, T. C., et al. (2019). Daily characteristics of Central African rainfall in the REMO model. *Theoretical and Applied Climatology*, *137*(3–4), 2351–2368. https://doi.org/10.1007/s00704-018-2745-5

Washington, R., James, R., Pearce, H., Pokam, W. M., & Moufouma-Okia, W. (2013). Congo Basin rainfall climatology: Can we believe the climate models? *Philosophical Transactions of the Royal Society B: Biological Sciences*, *368*(1625), 20120296. https://doi.org/10.1098/rstb.2012.0296

Weber, T., Cabos, W., Sein, D. V., & Jacob, D. (2022). Benefits of simulating precipitation characteristics over Africa with a regionally-coupled atmosphere–ocean model. *Climate Dynamics*, *60*(3–4), 1079–1102. https://doi.org/10.1007/s00382-022-06329-7

Weber, T., Haensler, A., Rechid, D., Pfeifer, S., Eggert, B., & Jacob, D. (2018). Analyzing regional climate change in Africa in a 1.5, 2, and 3°C global warming world. *Earth's Future*, *6*(4), 643–655. https://doi.org/10.1002/2017ef000714

Wu, M., Nikulin, G., Kjellström, E., Belušić, D., Jones, C., & Lindstedt, D. (2020). The impact of regional climate model formulation and resolution on simulated precipitation in Africa. *Earth System Dynamics*, *11*(2), 377–394. https://doi.org/10.5194/esd-11-377-2020

Zou, L., & Zhou, T. (2016). A regional ocean–atmosphere coupled model developed for CORDEX East Asia: Assessment of Asian summer monsoon simulation. *Climate Dynamics*, *47*(12), 3627–3640. https://doi.org/10.1007/s00382-016-3032-8

21698996, 2024, 3, Downloaded from https://agupubs.onlinelibrary.wiley.com/doi/10.1029/2023JD039385 by Alfred Wegener Institut F. Polar- U. Meeresforschung Awi, Wiley Online Library on [30/10/2024]. See the Terms and Conditions (https://onlinelibrary.wiley.com/terms-and-conditions) on Wiley Online Library for rules of use; OA articles are governed by the applicable Creative Commons License